Global seasonal variations of midday planetary boundary layer depth from CALIPSO space-borne LIDAR

Erica L. McGrath-Spangler,[1,2] and A. Scott Denning[3]

Received 9 October 2012; revised 14 January 2013; accepted 17 January 2013.

[1] We present a new global analysis of the depth of the planetary boundary layer (PBL) and consider regional variations throughout the year. PBL depth is estimated from the vertical variance of CALIPSO space-borne LIDAR backscatter associated with aerosol and shallow clouds during midday satellite overpasses and is only retrieved in the absence of optically thick clouds. The resulting analysis of over 100 million retrievals per year is therefore only a sample with higher frequency over deserts and other regions of strong subsidence, and lower frequency over regions of deep convection such as the ITCZ, tropical rainforests, and the Asian Monsoon.

[2] The mean of sampled PBL depths ranges from 500 m over cold oceans to more than 3000 m over hot deserts. The seasonal cycle of analyzed PBL depth is stronger over land than over water, and seasonality over land and midlatitude oceans is of opposite sign. Wintertime storm tracks and stratocumulus regions over subtropical oceans are prominent features of the analysis. Although evaluation of the new analysis is difficult due to previous sparse sampling by other methods, comparison of LIDAR-retrieved PBL depth with data collected by commercial aircraft generally shows good agreement.

Citation: McGrath-Spangler, E. L., and A. S. Denning (2013), Global seasonal variations of midday planetary boundary layer depth from CALIPSO space-borne LIDAR, *J. Geophys. Res. Atmos.*, *118*, doi:10.1002/jgrd.50198.

1. Introduction

[3] The planetary boundary layer (PBL) is the turbulent layer closest to the Earth's surface and is crucial to surface-atmosphere exchanges of energy, moisture, momentum, carbon, and pollutants. It is critical to understand the processes controlling its depth in order to adequately explain many of the weather, climate, and air pollution problems that scientists face today. With a midday depth over land of about 1–2 km, however, measuring the PBL top in situ is not a trivial endeavor. Therefore, observations of PBL depth are sparse [*Seibert et al*., 2000; *Jordan et al*., 2010; *McGrath-Spangler and Denning*, 2012], and no observation-based global PBL climatology exists [*Seidel et al*., 2010].

[4] Although many studies have successfully investigated PBL depth using radiosondes during field campaigns [e.g., *Johnson et al*., 2001; *Liu and Liang*, 2010], radiosondes are not necessarily deployed at ideal times for evaluating daytime PBL depth (e.g., morning and evening over North America). In addition, radiosondes (which are considered by many to be the gold standard of PBL depth measurements), even if launched at ideal times, may differ from the space/time average by up to 40% [*Stull*, 1988; *Angevine et al*., 1994; *White et al*., 1999]. *Stull* [1988], in particular, does not recommend determining PBL depth from a single rawinsonde for exactly this reason.

[5] Multiple methods are available to determine the depth of the PBL, but these estimates provide differing results and no standard PBL height definition exists [*Seidel et al*., 2010; *Ao et al*., 2012]. *Seidel et al*. [2010] examined radiosonde observations using seven different methods and found that in one analyzed profile, five different values of the PBL depth were found with differences over a factor of 10 depending on which definition was used. In their study, *Seidel et al*. [2012] found multiple sources of uncertainty when evaluating rawinsonde soundings, sometimes as much as 50%. These results and many others show that comparisons of PBL depth measurements depend upon the definition of PBL depth used and the instrument used to retrieve it [e.g., *Seibert et al*., 2000; *Wiegner et al*., 2006; *Mattis et al*., 2008; *Seidel et al*., 2010].

[6] There have been a few, limited scale studies examining PBL processes using space-based remote sensing [*Martins et al*., 2010]. *Guo et al*. [2011] for instance used radio occultation data from Global Positioning System (GPS) satellites in order to determine PBL depth over the oceans. These retrievals compare favorably with radiosonde data producing a correlation coefficient of about 0.82 [*Guo et al*., 2011]. The GPS data represent average mixing depth over tens to hundreds of kilometers because of the tangential path of the GPS signal through the atmosphere. *Ao et al*. [2012] also

[1]Universities Space Research Association, Columbia, Maryland, USA.
[2]Global Modeling and Assimilation Office, Code 610.1, NASA Goddard Space Flight Center, Greenbelt, Maryland, USA.
[3]Department of Atmospheric Science, 1371 Campus Delivery, Colorado State University, Fort Collins, Colorado, USA.

Corresponding author: E. L. McGrath-Spangler, GMAO, Code 610.1, NASA Goddard Space Flight Center, 8800 Greenbelt Road, Greenbelt, Maryland 20771, USA. (erica.l.mcgrath-spangler@nasa.gov)

2169-897X/13/10.1002/jgrd.50198

performed an analysis using GPS data to produce a global climatology of PBL heights and compared their product to meteorological re-analysis. PBL depth can be determined through cloud layers using the radio occultation data but only with relatively coarse horizontal resolution [*Guo et al*., 2011; *Ao et al*., 2012]. With its finer horizontal resolution, space-borne LIDAR strongly complements the GPS dataset.

[7] Space-borne LIDAR is sensitive to atmospheric aerosols and boundary layer clouds that can be used to identify the PBL top and has been used to provide information about the depth of the layer. It is a valuable tool in observing PBL depths on multiple platforms [*Ao et al*., 2012]. The LIDAR-In-Space Technology Experiment (LITE) flew for 9 days in September 1994 and was able to identify the PBL top by locating a sharp aerosol gradient [*Randall et al*., 1998]. Almost 10 years later, the Geoscience Laser Altimeter System (GLAS) was used to determine PBL depth over the oceans for October 2003 [*Palm et al*., 2005]. Most recently, *McGrath-Spangler and Denning* [2012] analyzed Cloud-Aerosol LIDAR and Infrared Pathfinder Satellite Observations (CALIPSO) data in order to determine PBL depths over North America during summertime. This study extends that method to produce a global analysis from June 2006 to December 2011.

[8] In our previous study, we showed that the CALIPSO LIDAR could be used to obtain quantitative estimates of the midday PBL depth in the absence of convective, optically thick clouds [*McGrath-Spangler and Denning*, 2012]. We found much deeper PBL over land than over water, a very deep PBL over the semiarid Southwestern United States, and a shallower layer over Midwestern farmland. Shallower PBL depths were evident off the California coast associated with cold water, stratocumulus clouds, and overlying subsidence. Mixing over boreal Canada was relatively deep, associated with the long summer days and high Bowen ratios observed in that region. The algorithm had reduced retrieval rates in regions with a high frequency of midday convection since the LIDAR aboard the CALIPSO satellite cannot penetrate optically thick clouds and a higher retrieval rate in regions with overlying subsidence reducing deep convection. The sampling error of the algorithm was greater over land than over the ocean.

[9] The LIDAR PBL depth algorithm compared well to the Modern-Era Retrospective analysis for Research and Applications (MERRA) with much of the continental United States within 25% of the reanalysis. Large differences occurred over the American Southwest, the boreal forests, and over the oceans. An additional analysis comparing CALIPSO PBL depths to PBL depths measured from aircraft temperature profiles showed that increasing the number of observations improved agreement between the two. These favorable results motivated this spatially and temporally expanded study covering the globe and the full year.

[10] The CALIPSO observations have the potential to expand our knowledge about PBL processes by providing a dataset to which both modelers and observers can compare PBL depth estimates. The following section provides a brief description of the method used to derive PBL depth from the CALIPSO satellite. Section 3 presents the results, and the final section provides conclusions.

2. Data and Methods

[11] The Cloud-Aerosol LIDAR with Orthogonal Polarization (CALIOP) instrument aboard the CALIPSO satellite is the first space-based LIDAR optimized for aerosol and cloud measurements and the first polarization LIDAR in space [*Winker et al*., 2007]. The LIDAR backscatter data are recorded at 532 nm (parallel and perpendicular polarization) and at 1064 nm. CALIPSO is part of the Afternoon (A-train) constellation of satellites with a 705 km sun-synchronous orbit. The A-train has an equator crossing time of about 1:30 P.M. local solar time and a 16 day repeat cycle [*Winker et al*., 2007, 2009]. The data used in this analysis are from versions 3.01 and 3.02 level 1B data available online from the Atmospheric Science Data Center at NASA Langley Research Center. The attenuated backscatter data used are at 30 m vertical and 0.33 km horizontal grid intervals below 8 km altitude and at reduced resolution aloft. Most observations occur between 1 and 2 P.M. local time except at high latitudes where longer summertime day lengths extend daytime observations. This analysis restricts observations to between Local Noon and 3 P.M. to ensure early afternoon observations. The method is the same as in *McGrath-Spangler and Denning* [2012] and described in more detail there, but a brief summary is presented here.

[12] The PBL depth is estimated using the attenuated backscatter data, and it is important to keep in mind that this is not a traditional, meteorologically based definition. Whereas the traditional definition uses temperature profiles from radiosondes to estimate the extent of turbulence by identifying the overlying inversion, this method identifies the aerosol-rich layer or the boundary layer capping clouds to estimate the extent of turbulence. The technique is based on the maximum variance technique of *Jordan et al*. [2010] and the idea by *Melfi et al*. [1985] that within the entrainment zone, there is a local maximum in the vertical standard deviation of the attenuated backscatter.

[13] *Jordan et al*. [2010] examined vertical profiles of retrieved 532 nm attenuated backscatter beginning at the surface and located the lowest occurrence of a local maximum in the vertical standard deviation (calculated over four adjacent altitude bins) collocated with a maximum in the attenuated backscatter itself. The algorithm is only applied to daytime LIDAR data but could potentially be extended to estimate the depth of the residual layer at night.

[14] *McGrath-Spangler and Denning* [2012] first horizontally averaged the profiles using a running mean over 60 km (corresponding to about 9 s) in order to improve the signal to noise ratio. The standard deviation at the vertical levels was then analyzed using a 120 m vertically sliding window from −2 km to 40 km (the extent of the profile) rather than discrete bins as was done by *Jordan et al*. [2010]. After computing the PBL depth estimate, the retrieved depths were horizontally averaged using a 60 km running mean in order to minimize the influence of outliers and to increase spatial continuity. This was then used as the final estimate of the PBL depth above ground level at each individual point.

[15] Additional deviations from *Jordan et al*. [2010] include automating the algorithm by restricting the retrieved depths to between 0.25 and 5 km depth (rejecting depths

outside that range), adding a check for surface noise, and removing profiles with overlying, attenuating clouds beneath which the LIDAR cannot adequately observe (using the threshold of *Okamoto et al*. [2007]).

[16] The algorithm has several limitations that must be considered when analyzing these data. First, optically thick clouds or aerosol layers attenuate the signal preventing observations of LIDAR attenuated backscatter below such a layer. This introduces a strong sampling bias relative to the time mean because cloudy conditions are not observed, and the orbital sampling of the instrument selects only midday conditions. Second, the algorithm sometimes detects an aerosol gradient from a previous day's residual layer rather than the current, shallower PBL, thereby overestimating the PBL depth. Additionally, multiple cloud layers are difficult to interpret, potentially causing a higher cloud layer to be identified rather than the top of the PBL. Furthermore, very shallow PBL depths cannot be retrieved due to surface noise complicating the retrieval. It is difficult to quantify these sources of error without a widespread independent measure of the PBL depth. However, with the increasing number of datasets, this type of analysis should be possible in the future.

[17] An additional consideration is that this method does not explicitly estimate the height of the temperature inversion but rather the height to which aerosols are lofted and clouds form, and this property must be kept in mind when choosing applications since these definitions are not necessarily equal [*Tucker et al*., 2009]. In addition to the weaknesses, the algorithm can fail due to the LIDAR not functioning properly (such as during a solar flare event).

3. Results

[18] Instantaneous values of PBL depth retrieved using the above method were averaged on to a $1.25° \times 1.25°$ grid covering the extent of the globe observed by CALIPSO. The data begin with the first observations of CALIPSO in June 2006 and extend through the end of 2011 with most grid boxes containing between 1000 and 10,000 retrieved PBL depth estimates meeting the criteria above. Temporal (over seasons) and spatial averaging was done in order to show general behavior, but the instantaneous values have been used for comparisons presented below. Only local midday values taken in conditions without optically thick clouds from other datasets should be used for evaluation and comparison.

3.1. Seasonal Discussion

[19] The retrieval rate maps in Figure 1 show the percentage of depths retrieved by the above algorithm compared to the total number of CALIPSO profiles available. This rate represents how often the algorithm failed due to attenuating, overlying convection or an unclear aerosol signature (i.e., a collocated local maximum in the attenuated backscatter and standard deviation is not found within the specified vertical range). It does not represent failures due to nonfunctioning LIDAR.

[20] Several features are evident in these maps. The Intertropical Convergence Zone (ITCZ) along the equator jumps out as a region of reduced retrievals due to high clouds associated with deep convection attenuating the LIDAR beam. Interpretable retrievals of PBL depth are made for less than 15% of CALIPSO profiles along the ITCZ and during

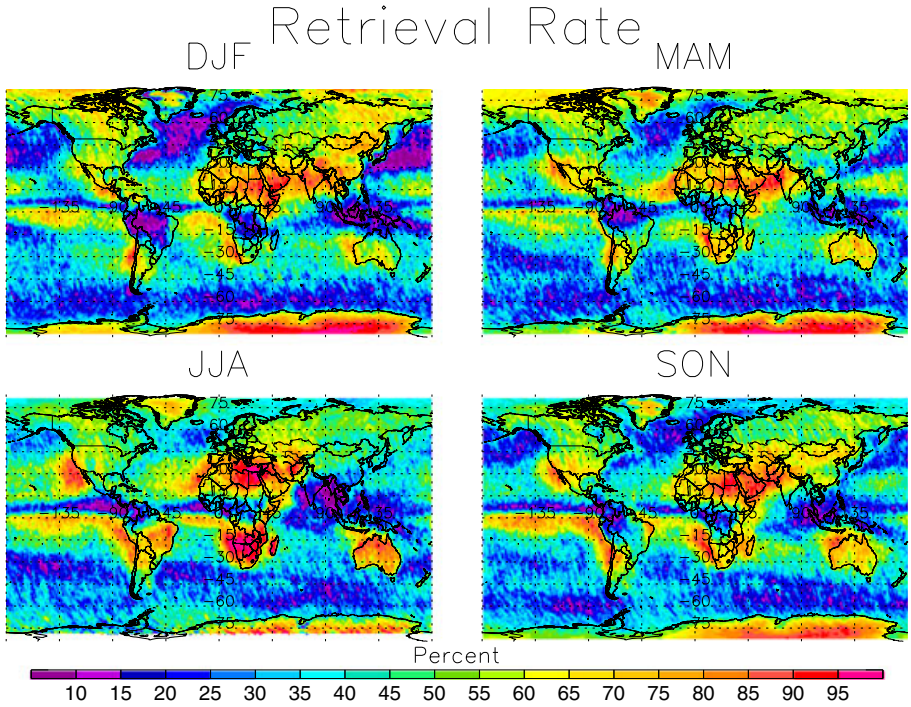

Figure 1. Ratio of the number of retrieved PBL depths to the total number of satellite profiles available times 100% gridded to $1.25° \times 1.25°$. Data are from June 2006 to December 2011 between local noon and 3 P.M. for conditions without optically thick clouds.

seasonal deep convection in tropical rainforests and monsoon regions. For instance, the Indian subcontinent shows high retrieval rates in the top two plots of Figure 1 (representing DJF [December, January, and February] and MAM [March, April, and May]) and again in the bottom right (representing SON [September, October, and November). However, during boreal summer, the Asian monsoon produces large regions of deep convection that then attenuate the LIDAR signal and cause the algorithm to fail, reducing the retrieval rates. Similarly, the affect of the rainy season on retrieval rates in the Amazon can be seen in Figure 1. The central Amazon rainforest experiences its rainy season anytime between southern hemisphere spring (SON) and fall (MAM) [*Marengo et al.*, 2001]. The retrieval rate during these months is reduced due to increased deep convection attenuating the LIDAR beam, with the lowest rates occurring in DJF.

[21] Within the subtropics, overlying subsidence suppresses deep convection and reduces the amount of signal attenuation. This allows interpretable retrieval of PBL depth for more than 85% of CALIPSO retrievals over deserts and marine stratocumulus clouds. In boreal winter, storm tracks associated with deep convection off the east coasts of North America and Asia show a reduction in retrieval rates. In general, this figure maps global regions of subsidence and convection and the seasonal evolution of both.

[22] Figure 2 shows the standard error of the mean (ratio of standard deviation to the square root of the number of observations) of the estimated CALIPSO PBL depths. The standard error of the mean provides a simple measure of the sampling error and an estimate of the uncertainty in the mean values but does not address systematic differences between these samples and the time mean over each grid cell that arise because the satellite samples only at midday in the absence of high clouds. As discussed above, this will introduce biases into the analysis. Specifically, it is expected that the sampled PBL depths will be greater than the actual time mean (over all times including the full diurnal cycle and over all weather conditions).

[23] In general, higher standard error of the mean (SEM) occurs over land where more heterogeneous PBL depths produce larger standard deviations. Regions with low retrieval rates (Figure 1) have relatively lower numbers of observations and therefore also have a higher SEM. These two factors produce the highest SEM over the tropical land and winter poles (North Pole in DJF and South Pole in June, July, and August [JJA]). Deep convection over the tropics associated with the rainy season and limited daytime observations due to polar night limit the number of observations and introduce more sampling error into the estimate. As in Figure 1, evidence of the seasonal cycle of the rainy season is apparent. The SEM is greatest over South America in DJF and in India it is greatest in JJA, showing that the satellite and algorithm are sensitive to climatic weather events.

[24] One of the great advantages of satellite data is its widespread coverage. Figure 3 presents the evolution of the retrieved PBL depth through the four seasons averaged to a 1.25° grid. As expected, deeper estimates of PBL depth are found over land than over water, and this difference is sensitive enough to identify islands in the Caribbean and the Galapagos. In addition, the PBL is deeper in the summer hemisphere and deepest over the deserts in Africa, the Middle East, Asia, and Australia in that season.

[25] In ocean regions, equatorial upwelling produces cold water that leads to shallow PBL depths. Stratocumulus cloud decks are evident off the west coasts of the subtropical continents and produce a deeper cloud-topped PBL.

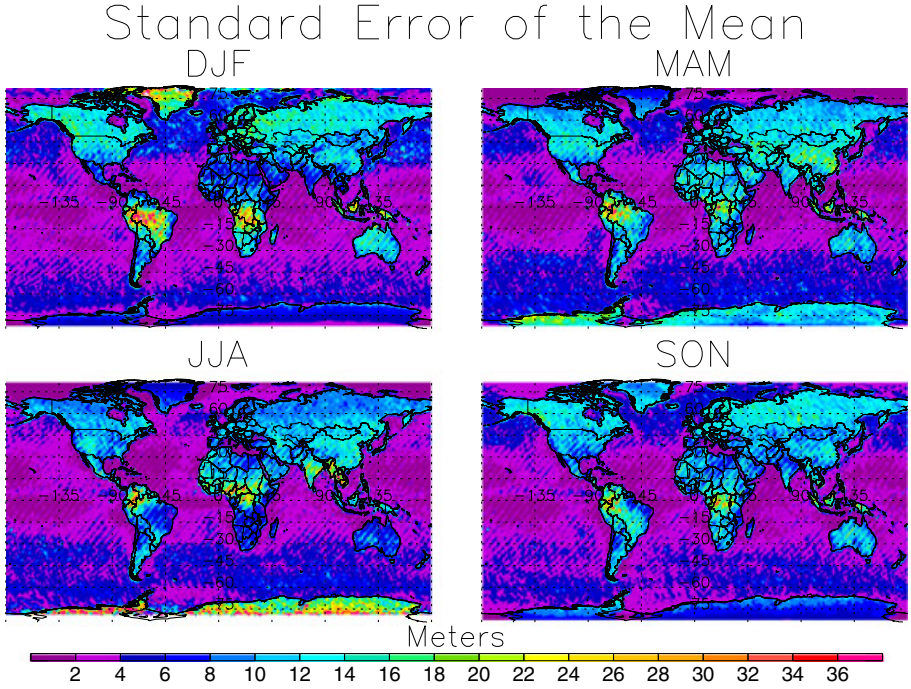

Figure 2. Standard error of the mean PBL depth gridded to 1.25° × 1.25°. Data are from June 2006 to December 2011 between local noon and 3 P.M. for conditions without optically thick clouds.

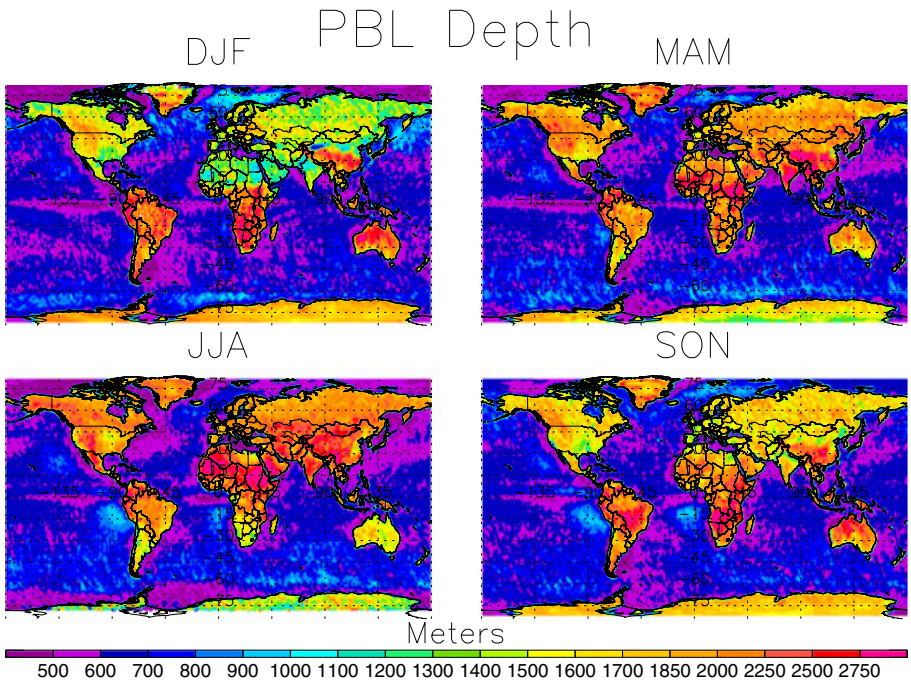

Figure 3. Mean PBL depth retrieved by the CALIPSO satellite gridded to 1.25° × 1.25°. Data are from June 2006 to December 2011 between local noon and 3 P.M. for conditions without optically thick clouds.

Additionally, the storm tracks off the east coasts of North America and Asia in winter produce regions of cold air traveling over warm water, creating instability. This leads to greater PBL depths that are visible in the DJF plot.

[26] The seasonal cycle of PBL depth detected by the CALIPSO satellite is apparent over India. During boreal winter when India is coldest, the retrieved depths are shallowest. In the months before the Asian monsoon (MAM in this plot), the temperatures are warmest and this is evident in the deepest retrieved depths. During the monsoon (JJA in this plot), the LIDAR cannot see through the deep convection and this biases the retrieval. The average depths therefore do not include any days with heavy precipitation and so the retrieved depths are relatively deep. In boreal fall, the temperature cools and the depths become shallower.

[27] Figure 4 shows the seasonal change in PBL depth. It is determined by subtracting the DJF mean PBL depth from the JJA mean PBL depth in Figure 3. Warmer colors indicate that the retrieved depth is deeper in boreal summer, while cooler colors indicate the depths are deeper in boreal winter. This map shows the differences in climate of various weather patterns such as storms, monsoons, subsidence, and temperature between the two seasons and their impact on PBL depth.

[28] The strong seasonal cycle in mixing depth over the deserts is striking, especially in the sub-tropics. The largest seasonal contrasts occur over the Sahara, Kalahari, Greater Australian, and Gobi deserts with seasonal changes well over a kilometer in some regions. In contrast, there is little variation over the tropics. The extratropical land generally shows deeper mixing during the summertime, and there is a distinct differentiation between the northern and southern hemispheres.

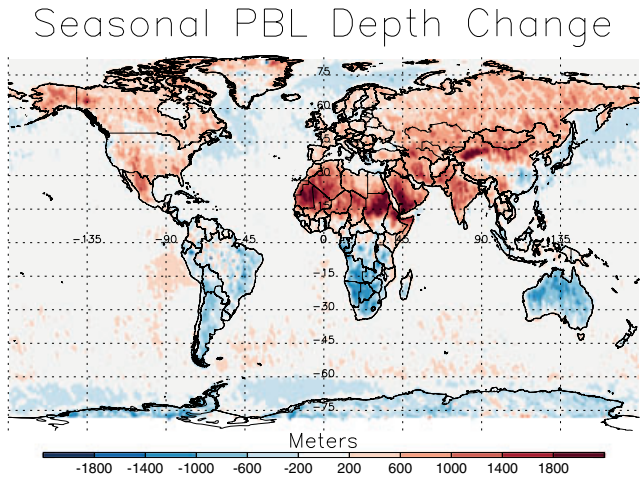

Figure 4. Seasonal changes in retrieved PBL depth found by subtracting DJF depths from JJA depths gridded to 1.25° 1.25°. Data are from June 2006 to December 2011 between local noon and 3 P.M. for conditions without optically thick clouds.

[29] CALIPSO-estimated PBL depths along the United States west coast are deeper during boreal winter than during the summer. This is consistent with the results of *Seidel et al.* [2010] who showed that the PBL depths over Oakland, CA were over 1000 m in winter and about 500 m during the summer. They argued that this was because of the subsidence inversions associated with the Pacific high-pressure system in the summer. In eastern China, the summer monsoon and its associated increase in deep convection limit the retrieval rate and will introduce a bias

into the retrieval. The times that are observed may experience an enhanced latent heat flux and consequently a decrease in the sensible heat flux and decreased PBL depths.

[30] The seasonal contrast over the oceans is much smaller than that over land indicating that the PBL depth is more homogeneous there. Where contrast does occur, it is generally opposite to the seasonal change over land. In the northern hemisphere, the storm tracks with deeper PBL depths during winter particularly stand out. However, in the Antarctic, south of 60°S, the oceanic PBL is deeper in the summertime than in the winter. This may be a result of the winter ice that extends out to this latitude providing a cold surface for the atmosphere minimizing any instability and producing shallow wintertime PBL depths.

[31] The average annual cycle of PBL depth detected by the CALIPSO satellite is shown in Figure 5. The top plot shows the average cycle over land and over water for the Northern Hemisphere (NH, latitudes greater than 23°N), the middle plot shows the same for the tropics (latitudes between 23°N and 23°S), and the bottom plot presents the Southern Hemisphere (SH, latitudes less than 23°S).

[32] In the NH and SH, the seasonal cycle over land is opposite to that over water with a 1 month lag in the NH. The largest seasonal cycle is over NH land with a percentage change of over 30%. In all three regions, the land PBL depth varies more throughout the year than over water. The PBL depth over tropical water exhibits only a 4% seasonal change indicating that the depth there is fairly consistent throughout the year and this agrees well with the results in Figure 4. The tropical land PBL depth has two maxima (April and September) during the shoulder seasons at higher latitudes. This is associated with a minimum in the winter hemisphere lowering the average PBL depth. In the shoulder seasons, both hemispheres have relatively deep PBL depths and allow the average PBL depth to remain high. Since the tropical NH contains more land, the impact of low SH wintertime PBL depths during boreal summer is minimized and the minimum in PBL depths during June is about 100 m deeper than the boreal winter minimum in December.

3.2. Comparisons to Aircraft PBL Depth

[33] Spatial and temporal separation between PBL depth observations must be considered when doing comparisons. *White et al*. [1999] found that the PBL depth can change by a kilometer in as little as 1 h, and it is well known that a point measurement may not be representative of the spatial average [e.g., *Angevine et al*., 1994; *White et al*., 1999]. Surface heterogeneity, variations in advection and subsidence as well as highly local conditions being measured by the instrument (e.g., a radiosonde traveling through a penetrating updraft rather than the predominant subsidence) contribute to these spatial and temporal differences. This sensitivity of the PBL depth must be taken into account when evaluating observing systems against each other and should be kept in mind for the following comparisons.

[34] Commercial aircrafts equipped with instruments to measure pressure, temperature, and height data produce the Aircraft Meteorological Data Reporting (AMDAR) dataset. These data provide atmospheric profiles during takeoff and landing and have been used to estimate the PBL depth by examining the temperature profile. The PBL was estimated by identifying the level of maximum vertical gradient of potential temperature as described by *Seidel et al*. [2010]. The CALIPSO satellite passed within 100 km and half an hour of one of these aircraft profiles over 4200 times representing 165 different airports.

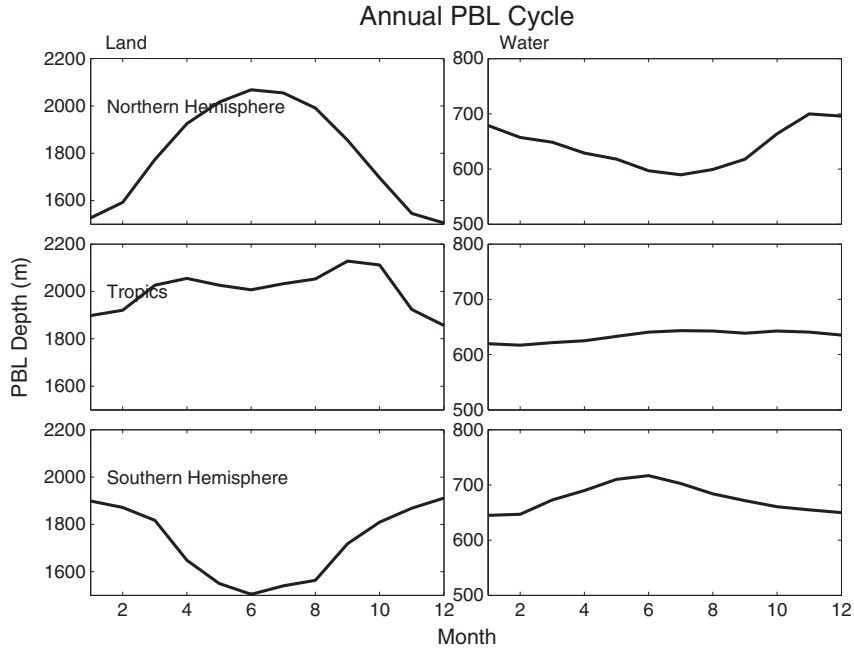

Figure 5. Average annual cycle of PBL depth over land (left) and over water (right) for the northern hemisphere (latitude greater than 23°N, top), the tropics (latitudes between 23°N and 23°S, middle), and the southern hemisphere (latitude less than 23°S, bottom). Data are from June 2006 to December 2011 between local noon and 3 P.M. for conditions without optically thick clouds.

[35] Figure 6 shows the ratio of the AMDAR-retrieved PBL depths to those estimated from the CALIPSO attenuated backscatter data times 100%. This figure only shows airports for which there were at least five observations and the CALIPSO profile occurred over land. Values greater than 100 indicate that the AMDAR retrieval was greater than the CALIPSO retrieval. About half of the airport locations agree within 25% of the CALIPSO estimates. The airport/CALIPSO ratios greater than ±40% (the space/time average error of radiosondes) [*Stull*, 1988; *Angevine et al*., 1994; *White et al*., 1999] have only a median of 14 collocated observations between the aircraft and satellite within the 5.5 years of this study (about one every 4.7 months). The largest disagreements occur in coastal regions where coastal dynamics such as land/sea breezes could potentially affect either the aircraft retrieval or the satellite retrieval, but not the other. Additionally, many airport locations in the semiarid southwestern United States show deeper aircraft-retrieved PBL depths. This could possibly be due to the heterogeneous terrain with airports predominately located in valleys. This introduces a geographical bias that would influence PBL depths and degrade their agreement. One must also keep in mind that the aircraft-retrieved PBL depths are estimated using the temperature profile while the satellite PBL depth estimate uses the attenuated backscatter and that these definitions are expected to produce differing results. No collocations occur in the Southern Hemisphere due to few aircraft observations of PBL depth. The paucity of AMDAR data over large areas of the world reinforces the relevance of satellite estimates of PBL depth that are more globally distributed.

[36] Figure 7 shows the percentage difference between the CALIPSO and AMDAR PBL depth estimates. The percentage difference is calculated by subtracting the values from CALIPSO from those of the aircraft, dividing by the average of the two, and then multiplying by 100%. Positive values indicate that the aircraft estimates were higher and 0% indicates perfect agreement. Most locations had fewer than 20 spatio-temporal matches in the 5.5 year time span, but there were some locations with more than 100 collocations between the aircraft and satellite profiles. The locations with the worst agreement occurred with relatively few collocations (less than 10), and as the number of collocations increases, the amount of agreement tends to increase as well. This implies that at least some of the disagreement is random and can be averaged out with enough data. Over 72% of stations have a percentage difference less than 40% (indicated by the dotted lines), which is the possible space/time average error of radiosondes [*Stull*, 1988; *Angevine et al*., 1994; *White et al*., 1999]. Thus, the favorable AMDAR to CALIPSO comparisons of *McGrath-Spangler and Denning* [2012] also apply globally and throughout the annual cycle.

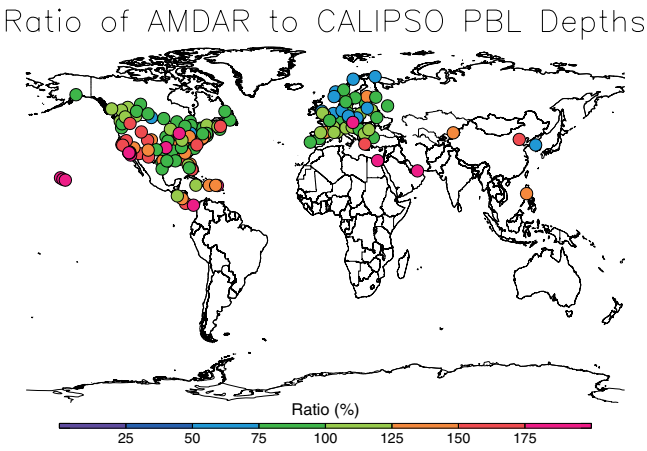

Figure 6. Ratio of estimates of PBL depth from commercial aircraft to CALIPSO at airport locations. Data are from June 2006 to December 2011 between local noon and 3 P.M. for conditions without optically thick clouds. The aircraft and satellite observations were made within 100 km and 30 min of each other.

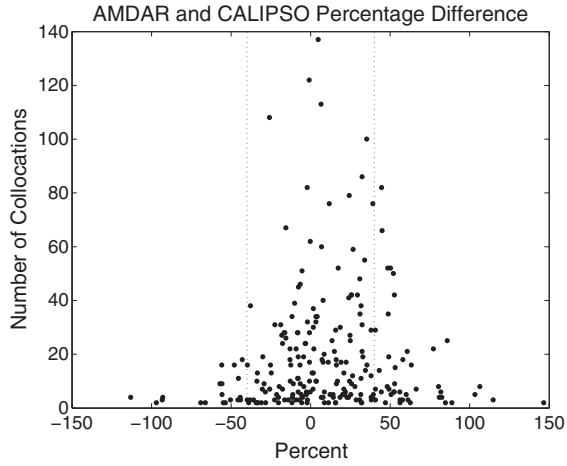

Figure 7. Scatter plot showing the relationship between the number of collocated observations between the commercial aircraft and satellite profiles and the percentage difference between these two systems. Data are from June 2006 to December 2011 between local noon and 3 P.M. for conditions without optically thick clouds. The aircraft and satellite observations were made within 100 km and 30 min of each other.

4. Conclusions

[37] Systematic estimation of the depth of the daytime PBL using LIDAR backscatter provides an unprecedented view of spatial and temporal variations of this important atmospheric property. Care must be used in the interpretation of the data because of the limited conditions under which the retrieval can be made. Optically thick clouds attenuate the LIDAR signal and make retrieval impossible, introducing a bias against conditions with deep convection. The potential exists for the residual layer from a previous day to be detected rather than a current shallower PBL, and surface noise inhibits the retrieval of very shallow PBL depths. Additionally, the presented algorithm detects changing features in the LIDAR attenuated backscatter, not the temperature inversion traditionally observed.

[38] In spite of these weaknesses, the high PBL depth retrieval rate results in millions of PBL depth observations. With an average global retrieval rate of about 45% and 850,000 daytime LIDAR profiles each day [*Winker et al*., 2009], over 100 million PBL depth estimates are retrieved

globally each year, producing an important dataset for constraining various atmospheric studies including those in air quality, cloud development, and the carbon budget. The global and seasonal analysis presented here shows that the algorithm is sensitive to climatological features such as the land/water contrast, the seasonal cycle, storm tracks, and monsoon seasons. Additionally, the water and land are shown to have opposite seasonal cycles due to instability over water in the wintertime. The largest seasonal change occurs over desert locations in Africa, Asia, and Australia with the largest uncertainty occurring over the tropics and winter poles. Increasing the number of collocated observations tends to improve agreement with aircraft temperature profiles.

[39] It is essential that general circulation and air quality models accurately represent boundary layer turbulence and exchange with the free troposphere. A global dataset of PBL depth is therefore needed, and estimates from CALIPSO satellite observations complement other datasets and fill a gap in current knowledge. There is great potential for using this dataset to improve simulated turbulence in atmospheric models and increase our understanding of PBL processes globally and accordingly our simulations of atmospheric constituents.

[40] **Acknowledgments.** This study was made possible in part due to the data made available to the National Oceanic and Atmospheric Administration by the following commercial airlines: American, Delta, Federal Express, Northwest, Southwest, United, and United Parcel Service. We would like to thank Nikisa Jordan and Mark Vaughan for their assistance with the CALIPSO data and the PBL depth algorithm. Additionally, we would like to thank three anonymous reviewers for their helpful comments. This research was supported by National Aeronautics and Space Administration grants NNX11AB87G and NNX08AV04H.

References

Angevine, W. M., A. B. White, and S. K. Avery (1994), Boundary-layer depth and entrainment zone characterization with a boundary-layer profiler, *Bound.-Lay. Meteorol.*, *68*(4), 375–385.

Ao, C. O., D. E. Waliser, S. K. Chan, J.-L. Li, B. Tian, F. Xie, and A. J. Mannucci (2012), Planetary boundary layer heights from GPS radio occultation refractivity and humidity profiles, *J. Geophys. Res.*, *117* (D16117), doi:10.1029/2012JD017598.

Guo, P., Y.-H. Kuo, S. V. Sokolovskiy, and D. H. Lenschow (2011), Estimating atmospheric boundary layer depth using COSMIC radio occultation data, *J. Atmos. Sci.*, *68*(8), 1703–1713, doi:10.1175/2011JAS3612.1.

Johnson, R. H., P. E. Ciesielski, and J. A. Cotturone (2001), Multiscale variability of the atmospheric mixed layer over the western Pacific warm pool, *J. Atmos. Sci.*, *58*, 2729–2750.

Jordan, N. S., R. M. Hoff, and J. T. Bacmeister (2010), Validation of Goddard Earth Observing System-version 5 MERRA planetary boundary layer heights using CALIPSO, *J. Geophys. Res.*, *115*(D24), D24218, doi:10.1029/2009JD013777.

Liu, S., and X.-Z. Liang (2010), Observed diurnal cycle climatology of planetary boundary layer height, *J. Climate*, *22*(21), 5790–5809, doi:10.1175/2010JCLI3552.1.

Marengo, J. A., B. Liebmann, V. E. Kousky, N. P. Filizola, and I. C. Wainer (2001), Onset and end of the rainy season in the Brazilian Amazon basin, *J. Climate*, *14*(5), 833–852.

Martins, J. P. A., J. Teixeira, P. M. M. Soares, P. M. A. Miranda, B. H. Kahn, V. T. Dang, F. W. Irion, E. J. Fetzer, and E. Fishbein (2010), Infrared sounding of the trade-wind boundary layer: AIRS and the RICO experiment, *Geophys. Res. Lett.*, *37*(24), L24806, doi:10.1029/2010GL045902.

Mattis, I., A. Ansmann, U. Wandinger, J. Preißler, P. Seifert, and M. Tesche (2008), Ten years of multiwavelength Raman lidar observations of free-tropospheric aerosol layers over central Europe: Geometrical properties and annual cycle, *J. Geophys. Res.*, *113*, D20202, doi:10.1029/2007JD009636.

McGrath-Spangler, E. L., and A. S. Denning (2012), Estimates of North American summertime planetary boundary layer depths derived from space-borne lidar, *J. Geophys. Res.*, *117*(D15101), doi:10.1029/2012JD017615.

Melfi, S. H., J. D. Spinhirne, S.-H. Chou, and S. P. Palm (1985), Lidar observations of vertically organized convection in the planetary boundary layer over the ocean, *J. Clim. Appl. Meteorol.*, *24*(8), 806–821.

Okamoto, H., et al. (2007), Vertical cloud structure observed from shipborne radar and lidar: Midlatitude case study during the MR01/K02 cruise of the research vessel Mirai, *J. Geophys. Res.*, *112*, D08216, doi:10.1029/2006JD007628.

Palm, S. P., A. Benedetti, and J. Spinhirne (2005), Validation of ECMWF global forecast model parameters using GLAS atmospheric channel measurements, *Geophys. Res. Lett.*, *32*(22), L22S09, doi:10.1029/2005GL023535.

Randall, D. A., Q. Shao, and M. Branson (1998), Representation of clear and cloudy boundary layers in climate models, in Clear and Cloudy Boundary Layers, edited by A. A. M. Holtslag, and P. G. Duynkerke, pp. 305–322, Royal Netherlands Academy of Arts and Sciences, Amsterdam.

Seibert, P., F. Beyrich, S.-E. Gryning, S. Joffre, A. Rasmussen, and P. Tercier (2000), Review and intercomparison of operational methods for the determination of the mixing height, *Atmos. Environ.*, *34*(7), 1001–1027.

Seidel, D. J., C. O. Ao, and K. Li (2010), Estimating climatological planetary boundary layer heights from radiosonde observations: Comparison of methods and uncertainty analysis, *J. Geophys. Res.*, *115* (D16), D16113, doi:10.1029/2009JD013680.

Seidel, D. J., Y. Zhang, A. C. M. Beljaars, J.-C. Golaz, A. R. Jacobson, and B. Medeiros (2012), Climatology of the planetary boundary layer over the continental United States and Europe, *J. Geophys. Res.*, *117*, D17106, doi:10.1029/2012JD018143.

Stull, R. B. (1988), An Introduction to Boundary Layer Meteorology, 666 pp., Kluwer Academic Publishers, Norwell, MA.

Tucker, S. C., W. A. Brewer, R. M. Banta, C. J. Senff, S. P. Sandberg, D. C. Law, A. M. Weickmann, and R. M. Hardesty (2009), Doppler lidar estimation of mixing height using turbulence, shear, and aerosol profiles, *J. Atmos. Ocean. Tech.*, *26*(4), 673–688, doi:10.1175/2008JTECHA1157.1.

White, A. B., C. J. Senff, and R. M. Banta (1999), A comparison of mixing depths observed by ground-based wind profilers and an airborne lidar, *J. Atmos. Ocean. Tech.*, *16*(5), 584–590.

Wiegner, M., S. Emeis, V. Freudenthaler, B. Heese, W. Junkermann, C. Münkel, K. Schäfer, M. Seefeldner, and S. Vogt (2006), Mixing layer height over Munich, Germany: Variability and comparisons of different methodologies, *J. Geophys. Res.*, *111*(D13), D13201, doi:10.1029/2005JD006593.

Winker, D. M., W. H. Hunt, and M. J. McGill (2007), Initial performance assessment of CALIOP, *Geophys. Res. Lett.*, *34*(19), L19803, doi:10.1029/2007GL030135.

Winker, D. M., M. A. Vaughan, A. Omar, Y. Hu, K. A. Powell, Z. Liu, W. H. Hunt, and S. A. Young (2009), Overview of the CALIPSO mission and CALIOP data processing algorithms, *J. Atmos. Ocean. Tech.*, *26*(11), 2310–2323, doi:10.1175/2009JTECHA1281.1.